THE CENTRAL REGION FOR COMPACT CYCLOTRONS

G. Bellomo

University of Milan - LASA
Via F.lli Cervi 201, 20090 Segrate (MI), Italy.

ABSTRACT

The main design features of the central region for compact cyclotrons are presented with emphasis on the phase space matching, i.e. beam quality.

Specific characteristics and problems of the superconducting cyclotrons and of the axial injection of the beam from external ion sources are examined.

1. INTRODUCTION

The design of the central region for compact cyclotrons has been covered extensively in the literature, but no attempt will be made here to list all the relevant papers devoted to the many aspects of the subject.

There is a general comprehensive view[1] of the problems associated with the central region but it is still lacking a clear procedure for its design. This because the performances of the central region are essentially determined by the first few turns of the beams and many different and sometime contradictory requirements must be met in order to obtain the best beam quality.

In the following it is tried to separate the different issues in order of growing complexity to allow a clear identification of the problems and limitations of the central region.

2. GENERAL CONSIDERATIONS

2.1 The Constant Orbit Mode

The central region of the cyclotrons is normally operated in the constant orbit mode [2], i.e. all the ions, for a given harmonic mode h ($\omega_{RF} = h\ \omega_0$), follow the same trajectory independently of their charge to mass ratio q/A and of the magnetic field level B_0.

This condition can be assured if the following relation is verified

$$\frac{V}{\omega_0 B_0} = \text{const} \qquad (1)$$

where V is the peak voltage of the dee. A more general relation [2] allows to compare and scale, for a given h and dees structure, different central regions through the Reiser parameter

$$X = \omega_0\ B_0\ \frac{d^2}{V}$$

where V is the peak voltage of the dee and d is the minimum dee-ground distance.

The constant orbit mode is almost mandatory when the central region has many electrodes crossing the median plane and/or reduced clearances. The maximum voltage of the dees, for the given law, is reached on the focusing line of the cyclotron ($T/A = K_{foc}\ q/A$) and therefore an ion chosen along the focusing line is sufficient to design the central region, for the given harmonic mode h.

Note that the constant orbit mode operation cannot assure an equivalent dynamic for all the beams since isochronous fields and focusing properties do not scale exactly with the field level. Still the constant orbit mode of operation gives acceleration properties very similar in the first few turns for all the beams.

A drawback of the constant orbit mode is the need to scale down, from the maximum allowed value, the dee voltage V by a factor of the order of 4-5 or more. For internal ion sources this correspond to a reduction of the intensity I according to the relation $I \div V^{3/2}$.

For external ion sources the scaling law (1) must be applied also to the source voltage and, beside the output current scaling, there is a reduced transmission due to increased vacuum losses, stray field, increased beam envelope, space charge.

Cyclotrons with one 180^0 dee can easily operate at maximum voltage just moving the source or rotating the inflector [3]. For all the other cyclotrons the solution is to have many central regions, designed to operate in constant orbit mode, with a different total turn number for each harmonic mode.

2.2 Electric Field Evaluation

Three methods are used to evaluate the electric field in the central region:
- electrolytic tank [4]
- relaxation programs [5]
- magnetic analogue method [6]

The first two methods actually measure (electrolytic) or compute (relaxation) the potential distribution, while the last method allows the direct evaluation of the electric field E through a linear relation with a measured magnetic field B.

With the electrolytic tank (in a scale normally from 3:1 up to 5:1) the potential distribution is usually measured on the median plane and the electric field components are obtained through derivatives of the potential V. The E_z field component outside the median plane is calculated as

$$E_z = - z \left(\frac{\partial V^2}{\partial x^2} + \frac{\partial V^2}{\partial y^2} \right)$$

With a relaxation code the potential is computed everywhere and the electric field can be calculated by derivatives corrected to high orders although this feature is normally not used, i.e. linear E_z field component is assumed. The relaxation codes are taking over the other two methods due to the increased speed and storage capability of the computers. The tridimensional mesh is generally of the cubic type with mesh size of the order of 1 mm. The computed fields are accurate starting from 2-3 mm from the electrodes.

The general shape of the electric field distribution in the gap region can be evaluated with a two-dimensional relaxation code. The field distribution for a standard dee gap geometry are presented in fig. 1. Some general conclusion can be drawn:
- the basic shape of the electric field in the median plane can be described with a gaussian function[6] whose standard deviation can be easily parametrized with the width and the height of the gap.
- the E_z field component is quite linear over a region covering approximately 50% of the gap. A reduction of the gap height of the dee, often used for axial focusing, implies therefore an equivalent reduction of the beam height.
- axial-longitudinal coupling can be introduced if the beam size is larger than 50% of the vertical aperture of the gap, due to variations of the transit time with the axial displacement z.

2.3 Trajectory Computation

The codes[7] used to evaluate the beam dynamics normally integrate the standard equation $F=q(E+v\times B)$ using either a cylindrical coordinates system with θ as independent variable (normally 2° step) or a cartesian one using τ (the step $\Delta\tau$ is a small fraction of the RF period).

For an internal ion source, owing to the importance of the transit time effect, the trajectories in the source-puller region are always evaluated as a function of the time.

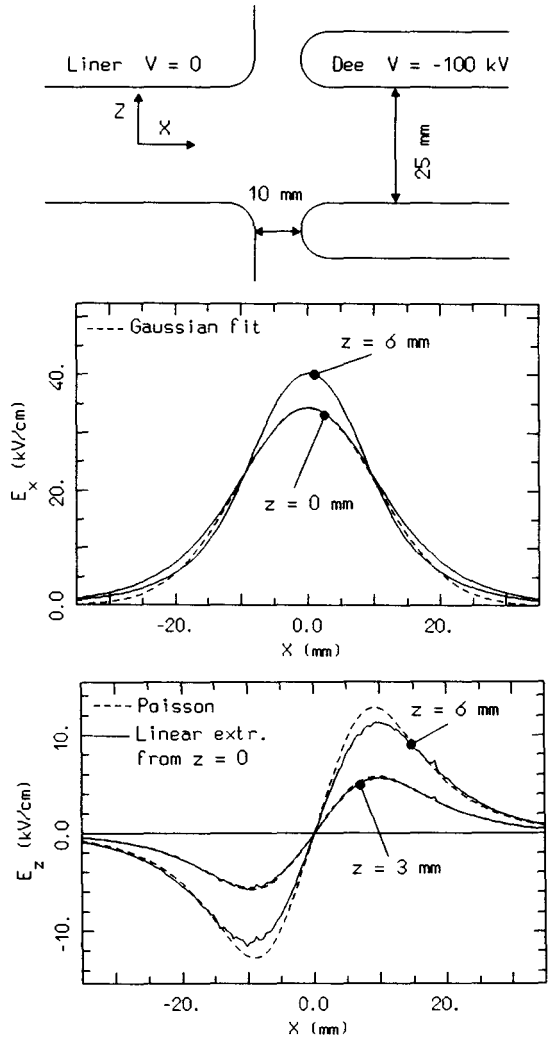

Fig. 1 - Schematic view of a bidimensional accelerating gap (top). Longitudinal electric field together with a gaussian fit (middle). Axial field component as given by the code and by extrapolation from midplane (bottom).

A linear motion in z is assumed consistently with the linearity of the E_z field component in the region occupied by the beam. The evaluation of E_z through second derivative of the potential is quite delicate since can introduce strong oscillations due to the noise in the potential data and it can be therefore used as a check of the midplane field evaluation.

Other computational schemes have been devised to utilize directly the potential data. In these methods[8] few equipotential lines for each gap (~10) are parametrized as simple curves (parabolas). The integration step is from the current position on an equipotential surface directly to the next equipotential surface.

Outside the central region (first 5-10 turns) the electric field is approximated with the gaussian shape or a δ function.

3. AXIAL FOCUSING

3.1 Magnetic Focusing

The amplitude C_N of the main harmonic of the field modulation (N is the number of sectors) close to the machine center has a radial dependence $C_N \cdot r^N$. Therefore for an isochronous field no axial magnetic focusing is provided for the first few turns. The addition in the center of the cone field, i.e. a small field bump (of the order of 10^{-2} of the main field) produces a positive field index and therefore axial focusing of the weak focusing type with a corresponding reduction of the radial focusing.

The cone field used for the Milan central region design and the variation of the radial and axial focusing frequencies are presented in fig. 2. The design goal for the cone field was to obtain a magnetic axial focusing of the order of $\nu_z = .1$ at low radii.

An additional effect of the cone field is to require an initial phase slip at injection (of the order of 20-30° RF) to reach isochronous acceleration beyond the cone region.

The cone field is however ineffective, for axial focusing, in the first turn and an additional focusing must be provided through the action of the accelerating electric field.

3.2 Electric Focusing

The axial focusing effect produced by the accelerating electric field has been analyzed in the case of a bidimensional gap geometry in historical papers[9].

Using the impulsive approach the focusing action can be given as

$$\frac{\Delta p_z}{p} = - z \left[\frac{h}{2r} \frac{qV}{T_c} \sin(\Phi) + \left(\frac{qV}{T_c} \right)^2 \cos^2(\Phi) \right]$$

where q is the charge, p is the momentum, T_c the energy of the ion at the centreline of the gap crossed at radius r, height z and RF phase Φ. The peak voltage applied to the gap is V and h is the harmonic mode. The validity of the formula is for $qV < T_c$. The first term of the right hand side is related to the time variation of RF electric field while the second term is due to the acceleration effects. The first term is generally dominating with the exception of $\Phi = 0$ or for extremely low injection energy.

With the assumption of a constant phase Φ the electric axial focusing variation can be cast in the form

$$\Delta \nu^2_z = h \sin(\Phi)/ (4\pi n)$$

where n is the turn number.

This formula, although quite approximated and not valid for the first turn of the central region, gives however an excellent scaling for the three main parameters namely harmonic number, RF phase and turn number.

Assuming for simplicity a phase dependence $\Phi \cdot 1/r$, for the cone field, the electric focusing scales as $n^{-3/2}$ and therefore it becomes quickly irrelevant after the first few turns.

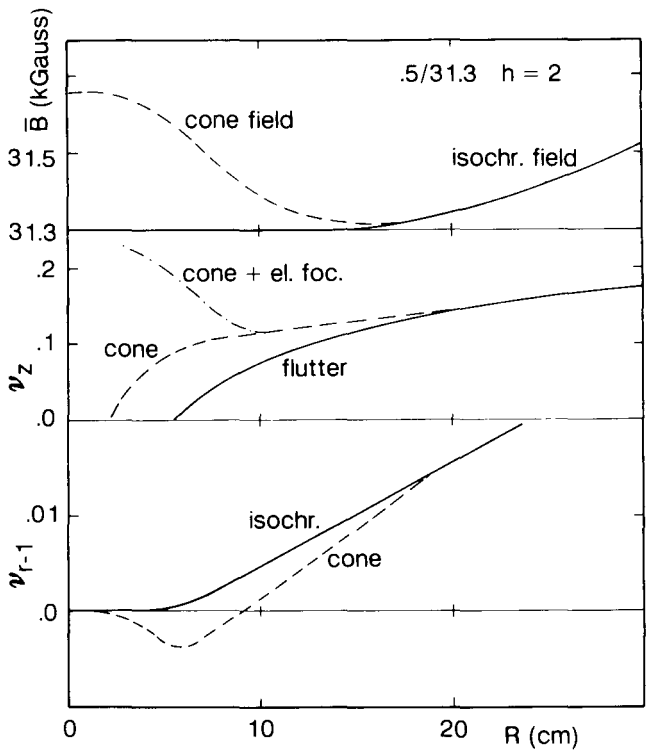

Fig. 2 - Isochronous and cone field for the central region of the Milan cyclotron (top). Axial focusing frequencies with the cone field and the electric focusing (middle). Radial focusing frequencies (bottom).

For the case of a tridimensional geometry of the gap, as in the case of posts on one or both sides of the gap, a general analysis[10], still based on the impulsive approach, gives the following relation

$$\frac{1}{f_x} + \frac{1}{f_z} = - \frac{h}{2rT_c} \frac{\partial(\Delta T)}{\partial \Phi}$$

where ΔT is the energy gain of the gap located at r and T_c is the energy at the gap center. Directly in term of focusing frequencies and turn number the equivalent formula is

$$\Delta \nu^2_r + \Delta \nu^2_z = \frac{h \sin(\Phi)}{4 \pi n}$$

with the implicit assumption of maximum energy gain for $\Phi = 0$ This formula show the possibility to obtain maximum energy gain and axial focusing by properly shaping the gap (asymmetries and posts).

A complete analysis[11] using the same approximation and generalized to all possible shape of the dees show that:

- a term must be added depending on the dee azimuthal extension and harmonic number
- there is an additional term for spiral dees (normally used in superconducting cyclotrons)
- there is the possibility of radial instability

Numerical and analytical results concerning different gap geometries can be found in References 10-12 and can be summarized as follows:

i) to increase the axial focusing
- decrease the gap height
- decrease the gap height only on the entrance side
- place two symmetric pillars on the exit side of the gap

ii) to decrease of the axial focusing
- increase the gap height
- place pillars on both side of the gap

3.3 Axial Phase Space

The central region designed for the Milan superconducting cyclotron[13], presented in fig. 3, is a quite elaborate example of dee shaping. Gap deformations were required to center properly the beam owing to the constrains of on-axis injection. In addition a strong vertical focusing was required at the inflector exit to match the small vertical beam size (~ 4 mm) and the large emittance (~ 500 mm mrad) to the cyclotron acceptance. The black areas and the cross-hatched areas correspond to post located on the dees or dummy dees while the horizontal hatched area and the dotted areas indicate a vertical reduction of the nominal gap (30 mm) to 16 mm and 20 mm respectively.

The electric field components, with the suppression of the time modulation, are presented in fig. 4 for the first turn of the central ray. The effects of the dees shaping on the first half turn are clearly visible. With specific regard to the axial focusing, a strong enhancement of the E_z field component has been obtained in the 1st and 3rd gap and an almost complete suppression in the 2nd gap.

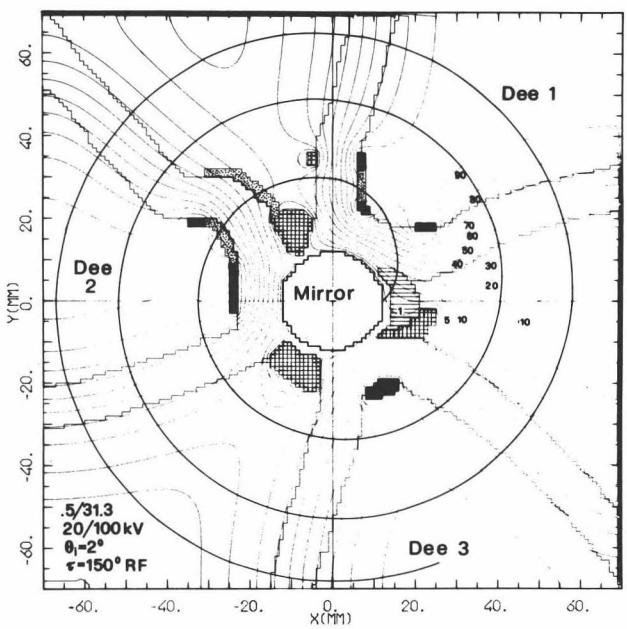

Fig. 3 - Central region geometry for the Milan superconducting cyclotron. The central ray is plotted together with the equipotential lines (all dees set at 100 kV).

Particular care has been devoted to reduce the phase dependence of the axial electric focusing as can be seen in fig. 5 where the trajectory of ions leaving the inflector with an axial displacement or axial divergence are plotted for three different starting times.

The eigenellipses at the inflector exit and the matched beam envelope for the central ray are presented respectively in fig 6 and fig 7. Although quite reduced the phase dependence of the axial focusing is still significant.

The phase dependence of the axial focusing is generally more critical in the case of internal ion source and high harmonic number[14].

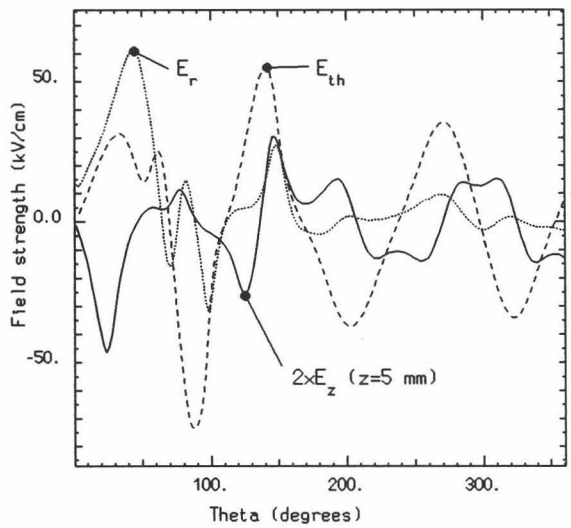

Fig. 4 - Electric field components, without the time modulation, along the central ray path for the first turn.

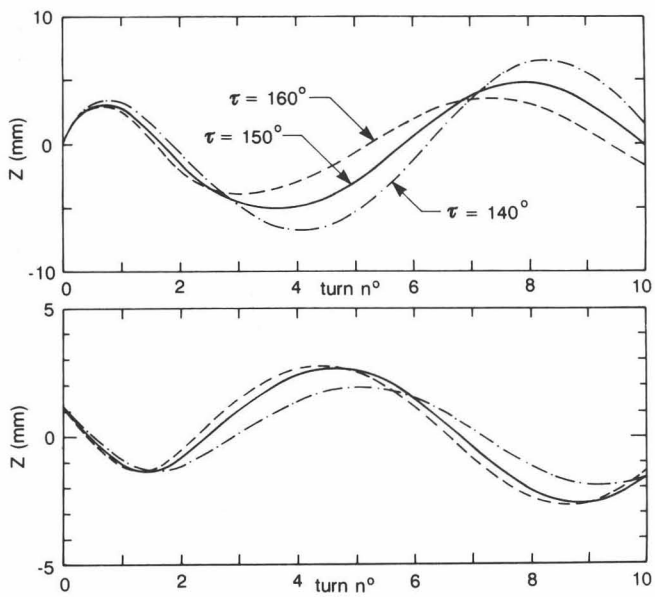

Fig. 5 - Linear vertical motion, for three starting times, for initial divergence (top) and displacement (bottom).

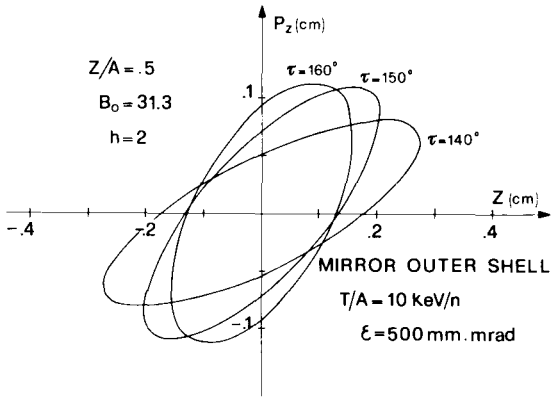

Fig. 6 - Axial eigenellipses for three starting times at the inflector exit.

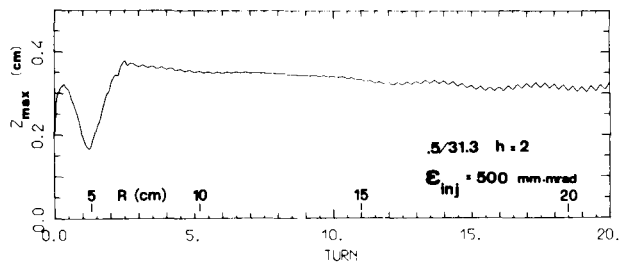

Fig. 7 - Axial envelope, for the central starting time, of a 500 mm mrad matched beam.

4. THE ACCELERATED EQUILIBRIUM ORBIT

The central ray of the accelerated beam should have, in analogy with the static equilibrium orbit (SEO), specific and unique characteristic and is therefore called accelerated equilibrium orbit (AEO).

One possible definition of the AEO, in addition to the requirement of maximum energy gain, is a smooth increase of the radius with the turn number i.e. the maximum centering compatible with the accelerating system.

The AEO can be determined with two equivalent methods. The first method compare in the space (r,p_r) the AEO with the SEO at the same energy therefore defining the radial phase space (x,p_x). Alternatively one can use the coordinates of the orbit center (x_c,y_c) loosely defined as the center of instantaneous curvature. For a rigorous definition of the orbit center see Ref. 15. For azimuthally symmetric magnetic field the relation are

$$x \simeq x \qquad y_c \simeq r\, p_x/p$$

when the AEO and the SEO are compared at $\theta=0°$.

The AEO is normally traced backward from outside the central region up to the 1st dee or 1st gap to obtain an indication of the position of the internal ion source or of the inflector. Qualitative informations can be obtained considering an ideal system namely an isochronous magnetic field (as given by the SEO) and an ideal impulsive δ acceleration at the gap crossing.

This ideal case is presented in fig. 8 for the Milan cyclotron characterized by three spiral dees, each one 60^0 wide. The coordinates of the AEO (respect to the SEO) are plotted at the center of the dees (valley) and of the dummy dees (hill) as a function of the turn number. The smoothness of the AEO is due to the perfect symmetry between the magnetic structure (3 sectors) and the accelerating system (3 dees). At the center of the dee the coordinates of the AEO are approximately

$$x \simeq 0 \qquad p_x \simeq \Delta r_{EO}$$

where Δr_{EO} is the radius increase of the SEO for the energy gain of a dee crossing.

The behaviour of the RF phase, plotted in fig. 8, shows that an isochronous field (defined by the SEO) does not produce the maximum energy gain in the first turns and this discrepancy increases for higher harmonic number and for increased dee voltages.

The adiabatic behaviour of the AEO therefore breaks down completely in the first turns of the central region.

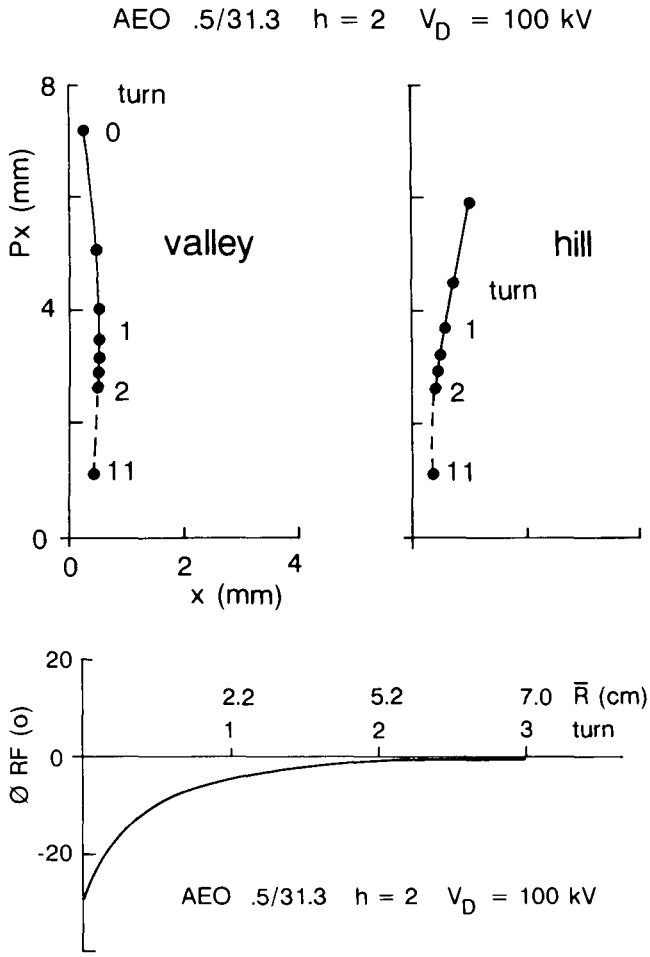

Fig. 8 - Accelerated equilibrium orbit for an ideal case as seen in the radial phase space at the center of hill and valley (top). RF phase slip of the AEO (bottom).

5. BEAM CENTERING

A general procedure for the design of the central region, once defined the accelerating structure (number and extension of the dees, harmonic mode, gap width and height), can be schematized as follows:

a) track backward the AEO up to the 1st dee or 1st gap
b) track forward from source or inflector up to the 1st gap or dee
c) match in energy, phase and coordinates by geometrical repositioning of the source, rotation of the inflector and dee or gap modification
d) check for axial focusing, clearances, phase acceptance, modify accordingly and restart from point b)

Generally speaking, when space is available, the design of the central region is determined essentially by the shape of the first two gap, i.e. the 1st dee. In tight situations or when particular constraints have to be met the design must involve all the 1st turn as exemplified in fig. 3 for the case of the Milan superconducting cyclotron where dees and gap shaping were required to match the AEO and to obtain axial focusing.

The match to the AEO is generally obtained within a few mm. This error can be easily corrected using a 1st harmonic of the magnetic field, produced by tunable coils, since the beam stays close to $\nu_r = 1$ for many turns in the central region.

For the Groningen cyclotron [16] an exceptionally high value of the off-centering (15 mm) has been corrected with strong field bumps ($\Delta B \simeq +140$ Gauss at r = 10 cm).

6. RADIAL-LONGITUDINAL COUPLING

The radial-longitudinal coupling for the motion of the beam in the cyclotron has been known from long time but only recently a general, and quite elaborated analysis[17], has been performed. A correlation in the plane (Φ_{RF},x'), in addition to the chromatic correlation $(x,\Delta E)$, must be introduced for a proper matching of the accelerated beam.

The need of this correlation can be easily demonstrated for the case of a uniform B field and a 180° dee system by requiring that a generic ion, with the same energy and position of the AEO at the gap crossing but with a small divergence $\delta=p_x/p$, should have, at the first order, the same energy gain per turn of the AEO.

Introducing the correlation (here $\nu_r=1$)

$$\Delta\phi_{RF} = -\frac{h}{\nu^2_r}\frac{p_x}{p}$$

the energy gain for the turn can easily be obtained by geometrical consideration (see fig.9) as

$$\Delta T = 2qV\cos(\Phi_{RF})\cos(\delta)$$

i.e. constant at the first order .

This leads to the definition[17,18] of the central position phase Φ_{cp} :

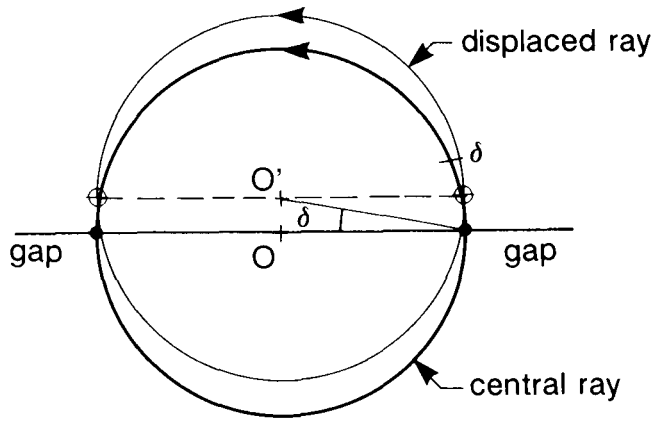

Fig. 9 - Example of the correlation (Φ_{RF},x') for the case of a 180° dee and a uniform field (see text).

$$\Phi_{cp} = \Phi_{RF} + \frac{h}{\nu^2_r}\frac{p_x}{p}$$

characterized by the following properties:

- it is a constant of the motion, on the turn, for all the ions of the radial phase space as opposed to the oscillation of Φ_{RF}
- it is the canonical coniugated of the energy E

It must be pointed out that at injection the two phases are quite different also for low harmonic number and therefore the correlation (Φ_{RF},x') is fundamental for beam matching. Outside the central region the two phases practically coincide due to the adiabatic damping of the divergences.

7. RADIAL PHASE SPACE

The ideal matched beam in the space (Φ,x,x') at injection and outside the central region is presented in fig 10. (from ref. 19). It has has the following characteristics:

- the central ray (i.e. the AEO) has the maximum energy gain
- the correlation (Φ_{RF},x') introduced at injection gives the same energy gain for each betatron phase space
- the energy spread for the given phase width is minimized ($\cos(\Phi_{cp})$ dependence)
- a phase compression (proportional to the transit time effect) is obtained.

There are however in reality many non linear effects which complicated the radial phase space matching and spoil the beam quality.

The correlation (Φ_{RF},x') for example is generally not linear, as in the case presented in fig. 11 for the Milan cyclotron and relative to a ± 130 mrad divergence respect to the AEO. The matching for these two ions is almost perfect already in the first turns as can be estimated by the crossing of the trajectories in fig. 11 and by the negligible energy spread. The correlation for this case should be $\Delta\tau_{RF} = \pm 15°$ while in reality is $\Delta\tau_{RF} = -14°, +9.5°$ respect to the $\tau_{RF} = 150°$ of the central ray.

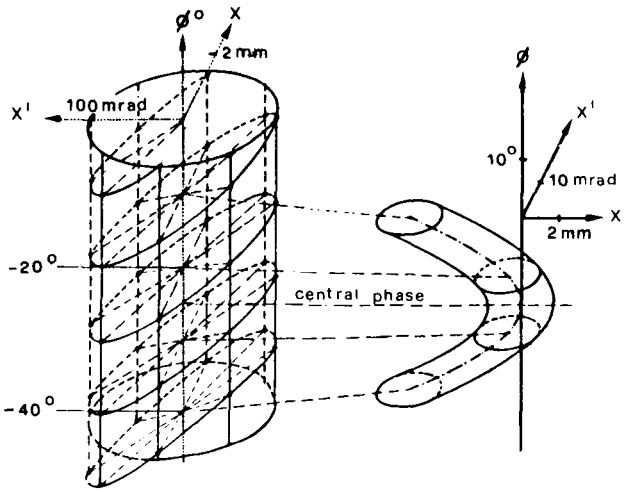

Fig. 10 - The ideal matched beam in the plane (x,x',Φ_{RF}) at injection (left) and outside the central region (right) [from ref. 19].

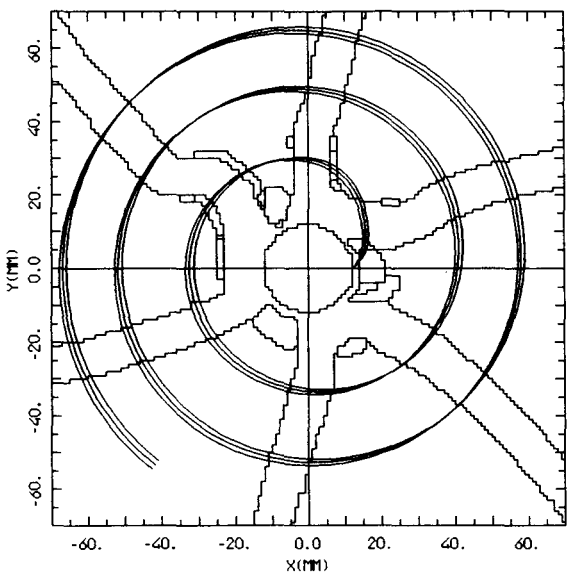

Fig. 11 - An example of proper matching using the correlation (Φ_{RF},x') for two ions with a ± 130 mrad divergence respect to the AEO.

A small linear correlation (Φ_{RF},x) is also required for an optimal matching of the order of $\Delta\tau_{RF} = \pm 5°$ for $x = \pm 1$ mm .

The effective radial focusing frequency in the first few turns can be estimated from fig. 11; the oscillations around $\nu_r = 1$ are quite pronounced in the first turn due to the electric focusing.

The evolution of the radial phase space, with the above mentioned correlations, is presented in fig. 12 as a function of the turn number for three different starting times. Deformation of the radial phase space are appreciable, although not severe, and become more pronounced for an extended range of starting phases.

The distortion of the radial phase space is still an indication of a non linear radial longitudinal coupling i.e. a phase dependence in ν_r due to the acceleration. For specific cases of accelerating system and high harmonic mode these distortion can become extremely severe[20]. A general analysis of these effects and examples are reported in ref 17-18.

The phase compression (always associated with transit time effects) for the case of the Milan central region is presented in fig. 13 together with the evolution of the RF phase of the central ray. In this case a compression of a factor 2 is obtained already at the 1st turn while hereafter the phase width is remarkably constant.

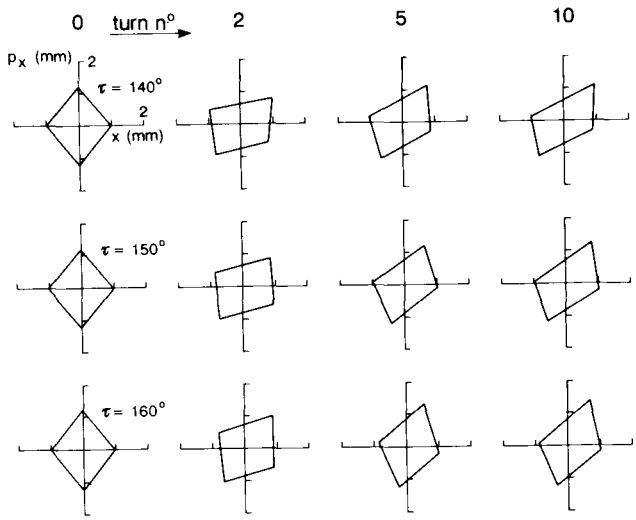

Fig. 12 - Evolution of the radial phase space, with the correlation (Φ_{RF},x') and (Φ_{RF},x), with the turn number for three starting times.

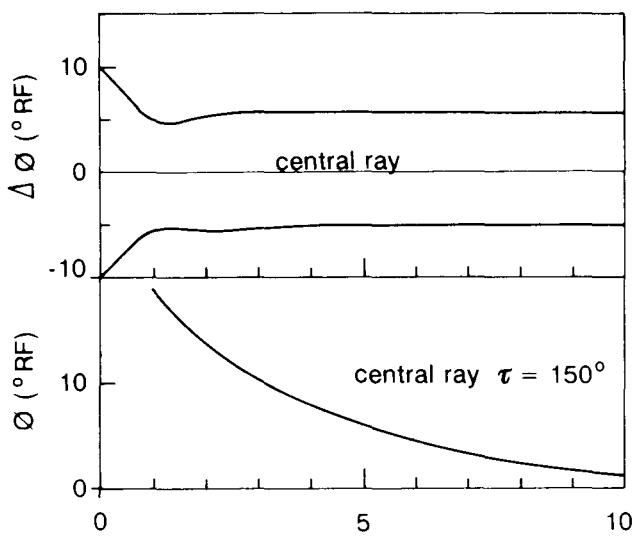

Fig. 13 - RF phase width as a function of the turn number n (top) and phase slip of the central ray (bottom).

8. PHASE SELECTION

The generally wide phase acceptance of the central region (of the order of 40-50° RF) imply a moderate internal beam quality and multiturn extraction in the case of internal ion source.

A phase selection system, to improve the poor beam quality of the extracted beam, is used in many cyclotrons[1-21] .

The main purpose of the phase selection system is to reduce the energy spread of the beam and/or the pulse length[1]. The two quantities are normally associated (E and Φ are coniugated variables) although the longitudinal phase space is essentially not linear ($\Delta E + \cos(\Phi_{RF})$) and dependent on the details of the acceleration process through all the machine[22].

Two methods are available namely the axial and radial phase selection.

Since in the first few turns the axial focusing (and the axial beam envelope) are phase dependent a two vertical slit system, with an object-image relation for the central phase, can provide phase selection.

The slits are normally separated by one half or one full vertical oscillation i.e. by 2.5 or 5 turns for an average focusing $\nu_z = 0.2$.

Slit apertures of the order of 1 mm are used and a phase width of ~ 5 RF (FWHM) can be obtained although with a strong reduction (of a factor 10) in beam intensity.

The same two slit system can be used also for the radial phase selection, owing to the radial longitudinal coupling (x,Φ) due to the phase dependent energy gain.

However a two slit system (180° apart since $\nu_r = 1$) in the first few turns performs poorly since:

- the betatron phase space has an envelope generally larger than the radial spread given by the phase dependent energy gain
- the proper variable is Φ_{cp}, and not Φ_{RF}, and therefore the energy gain has large oscillation in the first turn.

A two slit system at high turn numbers is more effective since the beam has ideally a distribution $\Delta r = \cos(\Phi)$ and the slit separation is of the order of 20 turns ($\nu_r = 1.025$). With slit aperture of ~ 1 mm it is possible to obtain a phase width, and intensity, comparable to the case of axial phase selection.

If the centering of the beam, at high turn number, is still phase depending it is possible to increase the phase selection. An exceptionally good phase selection of 1.4° RF (FWHM) has been reported[1] for such a case.

9. SUPERCONDUCTING CYCLOTRONS

The superconducting cyclotrons, from the point of view of the central region, can be characterized as compact cyclotrons with a very high magnetic field in the range 20-50 kGauss i.e. of the order of threetimes the field of room temperature cyclotrons.

To provide turn separation the accelerating system has the dees located in each valley with relatively high voltage (typically 100 kV).

There are problems associated with the transit time in the first few gaps since the Reiser parameter

$$\chi = (d/E)\ \omega\ B$$

increase quadratically with the field level being the factor (d/E) essentially a constant as given by the usual 100 kV dee-ground for a 1 cm of minimum distance. The high value of the χ parameter for the central region of superconducting cyclotron force to use low harmonic numbers (h=1 or h=2 for a three dee system) for the maximum turn case with a reduced accelration efficiency (50% for h=1).

The central region of superconducting cyclotrons is therefore very tight with a large number of posts, to limit the transit time effects,and reduced clearances. An extreme design example is the central region for the MSU K100 superconducting medical cyclotron[23] presented in fig. 14.

In addition the operation of a three dee system in the h=1 or h=2 harmonic modes requires a low capacitive coupling between the dees to avoid instability of the RF system. A partial shielding of the dee must therefore be provided[13] using additional post or the body of the source or inflector.

The central region is very tight[13,24] also in the case of axial injection: the reduced space available for the inflector limit the injection voltage to ~ 20-30 kV. Mirror and spiral inflector have been considered as inflectors with a preference for the latter since it requires lower operating voltages and therefore it is without sparking problems.

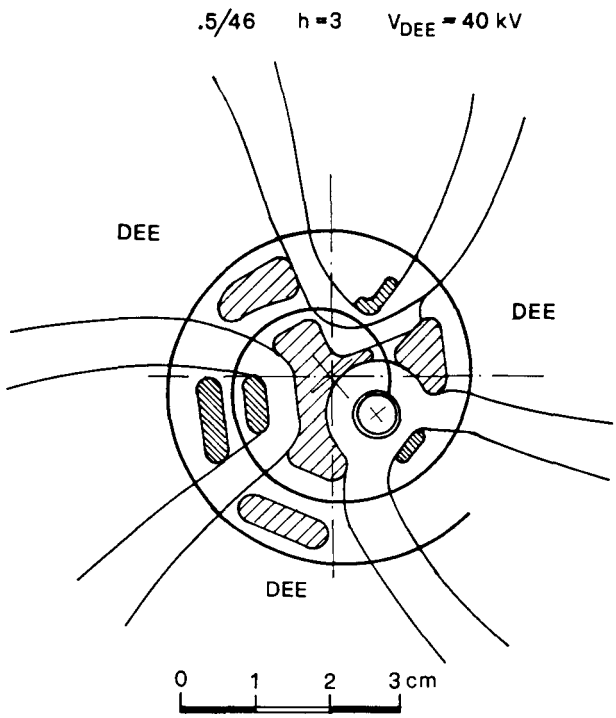

Fig. 14 - The central region of the MSU superconducting medical cyclotron.

The strong magnetic field along the axial injection path introduces additional problems:
- the transport and focusing of the beam along the axial path is quite difficult[25)]
- between the buncher and the inflector there is a severe debunching[26)] effect due to the high magnetic field and the relatively low injection voltage
- stray fields along horizontal beam line connecting the source to the axial line require a shielding.

10. AXIAL INJECTION

The axial injection of the beam from external ion sources has been quite a specialized feature for compact cyclotron up to the advent of the ECR ion sources[27)]. For a review of axial injection system see ref. 28.

Beside an improved operation of the cyclotron related to the better vacuum and charge selection, the axial injection has many advantages for the beam quality like:
- the injection at 10-20 kV reduce the effects related to the transit time in the 1st gap
- the phase width can be considerably reduced (up to 15-20° RF) with a bunching system
- the transversal phase space matching is possible using focusing elements along the axial beam line.

These theoretical advantages are however practically spoiled by the complexity of the matching due to the introduction of coupling between the phase spaces at different locations: source (if of the ECR type), injection path (with longitudinal magnetic field), inflector.

A zero emittance beam (parallel rays) originated inside the longitudinal magnetic field of the ECR source in the field free region after extraction has a transversal coupling emittance[29)] ε_c :

$$\varepsilon_x = \varepsilon_y \equiv \varepsilon_c = \pi \frac{r_s^2 B_s}{2 (B\rho)}$$

where r_s is the radius of the extraction hole, B_s the longitudinal field , $(B\rho)$ the beam rigidity after extraction.

In addition there is a correlation (x,p_y) and (y,p_x) $r_{14} = -r_{23} = \pm 1$ depending on the field orientation.

For an intrinsic emittance ε_o of the source, due to the transverse temperature, after extraction the beam has a total emittance ε_T

$$\varepsilon_T^2 = \varepsilon_o^2 + \varepsilon_c^2$$

The normalized intrinsic and total emittances of a typical ECR source operating at 10 GHz (B_s = .36 T) with r_s = 3 mm and transverse temperature kT = q·1eV is plotted in fig. 15 as a function of q/A together with the correlation coefficient.

The very good value of the intrinsic emittance is spoiled at high charge state by factors of 2-3 .

A scheme to complete decouple the transverse phase space using a skew quadrupole has been proposed and tested[30)].The intrinsic emittance can be recovered in one plane while in the other plane its value is twice the coupling emittance. Therefore the decoupled beam has emittances in the two planes different by factor 4-9.

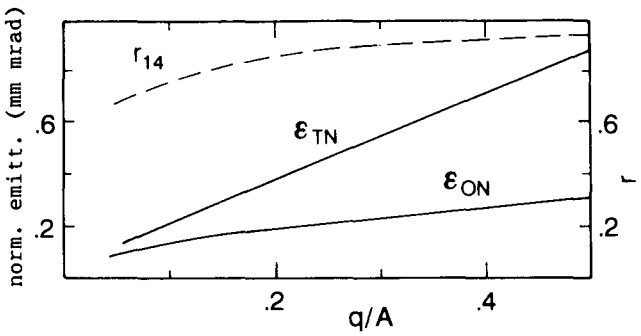

Fig. 15 - Intrinsic ε_{ON} and total ε_{TN} normalized emittances for a typical ECR source as a function of q/A (see text). The transverse correlation coefficient is also plotted.

The emittance increase and the transversal coupling at the median plane of the cyclotron due to the magnetic field along the axial injection path is a similar effect.

Analytical and numerical studies of the coupling characteristic of the inflectors has been done at many Laboratories.

The effects of all these couplings (source, axial path, inflector) is an injected beam with coupling between all the planes and increased value of the emittances.

The implication on the beam dynamic in the central region have not yet been analyzed ; these couplings apparently are not extremely severe judging from the results of the GANIL injector[31)].

Studies are ion progress to minimize these effects using skew quadrupole to introduce, for successive partial compensation, transversal coupling and minimize the emittance growth at the cyclotron[32)].

An elaborate solution (including space charge compensation) has been proposed for the axial injection in GANIL[33)].

The beam from the the ECR source is first decoupled an then a complete matching is obtained by introducing , with skew rotating quadrupoles, buncher and dipoles, the proper phase space correlations to obtain a fully decoupled beam after the inflector.

11. CONCLUDING REMARKS

The beam dynamic in the central region is well understood. Still the phase dependent effects, namely axial focusing and radial-longitudinal coupling, are quite difficult to manage for an ideal beam matching and the radial and axial beam quality is spoiled (precessional mixing).

The exploitation of ECR ion sources requires a complicated matching procedure for the axial injection of the beam to take full

advantage of the system. The studies in progress at many Laboratories will bring new understanding and therefore new possibilities to improve the beam quality.

Space charge effects, not treated in this paper, will become quite important in the future also for the machine dedicated to Nuclear Physics as exemplified by the GANIL case.

ACKNOWLEDGMENTS

The author gratefully acknowledges the fruitful discussions with many colleagues. Special thanks to M.P. Bourgarel, F. Marti, B. Milton and J.P. Shapira for their suggestions and for making available their results.

REFERENCES

1) H.G. Blosser - IEEE Trans. Nucl. Sci. NS-13 (1966), 1
H.G. Blosser - Proc. 5th Int Cycl. Conf. (Oxford 1969), 257
2) M. Reiser - Nucl. Instr. and Meth. NIM 18-19 (1962), 370.
3) D.J. Clark and C.M. Lyneis - Proc. 11th Int. Cycl. Conf. (Tokyo 1986), 499
4) S.J. Burger et al. - Proc. 10th Int. Cycl. Conf. (East Lansing 1984) ,63
5) C.J. Kost and F.W. Jones - RELAX3D , TRIUMF internal report TRI-CD-88-01 (1988)
6) N.Hazewindus et al. - Nucl. Instr. and Meth. NIM 118 (1974), 125
7) CYCLONE - MSU Internal report
8) P. Mandrillon - Report IPNO-GTA/85-01 -Orsay
S. Albrand et al. - Proc. 11th Int. Cycl. Conf. (Tokyo 1986),191
9) M.E. Rose - Phys. Rev. 53 (1938), 392
R.R. Wilson - Phys. Rev. 53 (1938), 408
B.L. Cohen - Rev. Sci. Instr. 24 (1953), 589
10) G. Dutto and M.K. Craddock - Proc. 7th Int. Cycl. Conf. (Zurich 1975), 271
11) M.M. Gordon and F. Marti - Part. Acc. 11 (1980), 161
12) M. Reiser - J. Appl. Phys. 42 (1971),4128
C.S. Han and M. Reiser - IEEE Trans. Nucl. Sci. NS-18 (1971), 292
13) G. Bellomo and L. Serafini - Proc.11th Int. Cycl. Conf. (Tokyo 1986), 507
14) J. Griffin and F. Marti - Proc. 10th Int. Cycl. Conf. (East Lansing 1984),48
15) H.L. Hagedoorn - Proc. 10th Int. Cycl. Conf. (East Lansing 1984), 271
16) W.K. van Asselt et al. - Proc. 9th Int. Cycl. Conf. (Caen 1981), 267
17) W.M. Shulte - EUT Thesis , Eindhoven (1978)
W.M. Shulte and H.L. Hagedoorn - IEEE Trans. Nucl. Sci. NS26 (1979),2388
W.M. Shulte and H.L. Hagedoorn - IEEE Trans. Nucl. Sci. NS26 (1979),2329
18) M.M.Gordon and F. Marti - Part. Acc. 12 (1982), 13
19) W.P. Lutter et al. - IEEE Trans. Nucl. Sci. NS-18 (1971), 321
20) J.L. Bolduc and G.H. Mackenzie - IEEE Trans. Nucl. Sci. NS-18 (1971), 287
G. Dutto et al. - Proc. 6th Int. Cycl. Conf. (Vancouver 1972),340
21) G.C.L. van Heusden - Thesis, Eindhoven (1976)
J. Reich et al. - IEEE Trans. Nucl. Sci. NS-26 (1979), 2007
S.J. Burger et al - Proc. 10th Int. Cycl. Conf. (East Lansing 1984), 67
22) M.M. Gordon - Proc 10th Int. Cycl. Conf. (East Lansing 1984), 279
23) H.G. Blosser - Proc. 10th Int. Cycl. Conf. (East Lansing 1984), 431
24) F. Marti and A. Gavalya - Proc. 11th Int. Cycl. Conf. (Tokyo 1986), 484
J.P. Shapira et al. - AGOR central region design, this Conference
25) G. Bellomo et al. - Nucl. Instr. Meth. NIM 206 (1983), 19
26) G. Bellomo - Proc. 11th Int. Cycl. Conf. (Tokyo 1986), 503
27) R. Geller - Proc. 11th Int. Cycl. Conf. (Tokyo 1986), 699
28) G. H. Ryckewaert - Proc. 9th Int. Cycl. Conf. (Caen 1981), 241
29) J.I.M. Botman and H.L. Hagedoorn - The beam emittance of cyclotrons with an axial injection system -Proc. EPAC Conf. (Roma 1988)
30) J.Reich et al - Partial beam decorrelation of sources - Proc. EPAC Conf. (Roma 1988)
31) M.P. Bourgarel et al. - Modification of the GANIL injector, this Conference
32) R. Baartman - Matching of ion sources to cyclotron inflectors - Proc. EPAC Conf. (Roma 1988)
J.I. Botman et H.L. Hagedoorn - Axial inflectors and the correlation between phase spaces, this Conference
33) A.R. Beck et al - Six-dimensional matching for axial injection into a cyclotron, this Conference